

## 2018 SNMMI Highlights Lecture: Oncology and Therapy, Part 2

Andrew Scott, MD, Director of the Department of Molecular Imaging and Therapy, Austin Health, and Head, Tumor Targeting Laboratory, Olivia-Newton John Cancer Research Institute, Melbourne, Australia

*From the Newsline Editor: The Highlights Lecture, presented at the closing session of each SNMMI Annual Meeting, was originated and presented for more than 30 years by Henry N. Wagner, Jr., MD. Beginning in 2010, the duties of summarizing selected significant presentations at the meeting were divided annually among 4 distinguished nuclear and molecular medicine subject matter experts. Each year Newsline publishes these lectures and selected images. The 2018 Highlights Lectures were delivered on June 26 at the SNMMI Annual Meeting in Philadelphia, PA. In this issue we feature part 2 of the lecture by Andrew Scott, MD, Director of the Department of Molecular Imaging and Therapy, Austin Health, and Head, Tumor Targeting Laboratory, Olivia Newton-John Cancer Research Institute (Melbourne, Australia), who spoke on oncology highlights from the meeting. The first part of the lecture appeared in the December issue of Newsline. Note that in the following presentation summary, numerals in brackets represent abstract numbers as published in The Journal of Nuclear Medicine (2018;59[suppl 1]).*

The first part of this lecture included an overview of reports and advances presented at the SNMMI 2018 Annual Meeting and highlighted specific presentations relevant to molecular probes for drivers of oncogenesis and to immunooncology, the latter focusing on molecular imaging of response and response criteria for immunotherapy, novel imaging probes, and the tumor immune microenvironment.

### Novel Imaging Targets in Cancer

We currently have a plethora of novel targets for development in cancer imaging. An extraordinarily large number of cell surface, intracellular, nuclear, and even stromal targets are available for exploration. Which ones we choose to pursue will depend on the questions we want to ask. Kardan et al. from Kettering Medical Center (OH), Cardinal Health Regulatory Sciences (Overland Park, KS), the University of California at Los Angeles, and Wright State University (Kettering, OH) reported on a “Comparison of  $^{99m}\text{Tc}$ -tilmanocept and  $^{99m}\text{Tc}$ -sulfur colloid for intraoperative lymphatic mapping and sentinel lymph node biopsy in breast cancer patients” [418]. This interesting presentation went beyond classic small particle-based approaches in sentinel node imaging by targeting the anti-CD206 mannose receptor with a technetium-labeled probe ( $^{99m}\text{Tc}$ -TM). The goals were to observe injection site clearance rates, sentinel lymph node uptake patterns, and patterns of locoregional lymph node drainage. The imaging

results, including numbers of lymph nodes identified intraoperatively, were similar with the 2 agents, although the  $^{99m}\text{Tc}$ -TM had some notable advantages. What is significant here is that we are actually looking at 2 different physiologic processes with the 2 agents. These authors were looking beyond patterns of locoregional lymph node drainage to assess clearance from the primary tumor itself (Fig. 1). It is exciting that they are looking beyond particles and trafficking to explore what is happening on a biologic basis within these nodes. This opens the potential for development of probes that can be more relevant to tumor-positive nodes as opposed to draining nodes.

Various interesting new probes were reported at this meeting. Hotta et al. from the National Center for Global Health and Medicine (Tokyo), Tohoku University (Sendai), and Tokyo Metropolitan Institute of Gerontology (all in Japan) reported on “Efficacy of 4’-[methyl- $^{11}\text{C}$ ]-thiothymidine (4DST) PET/CT before and after neoadjuvant therapy for predicting therapeutic responses in patients with esophageal cancer” [158]. This agent has been used as a cell proliferation imaging PET tracer that incorporates directly into DNA. The study included 23 patients with histologically diagnosed esophageal cancer who underwent 4DST and  $^{18}\text{F}$ -FDG PET/CT before and after neoadjuvant chemotherapy or chemoradiation. Again, the imaging results were quite similar, particularly before treatment, although the targets were different, with 4DST looking at DNA turnover (Fig. 2). Analysis showed that post-therapeutic 4DST  $\text{SUV}_{\text{max}}$  had the most accurate diagnostic performance for predicting responses. The authors concluded that 4DST PET/CT has a potential equal to or greater than  $^{18}\text{F}$ -FDG PET/CT to predict therapeutic responses to neoadjuvant therapy in esophageal cancer and that “higher uptake of 4DST after neoadjuvant therapy may indicate an inadequate response...and may be a promising marker to determine the appropriate therapeutic strategy for treating esophageal cancer.” I commend this group of researchers for exploring a very interesting targeting approach.

One of the advantages of having this widening range of available targets is the ability to select targets based on the specific biology of the cancer itself. Wei et al. from the Shandong Cancer Hospital and Institute (Jinan, China) reported on the “Relationship between clinicopathological



Andrew Scott, MD

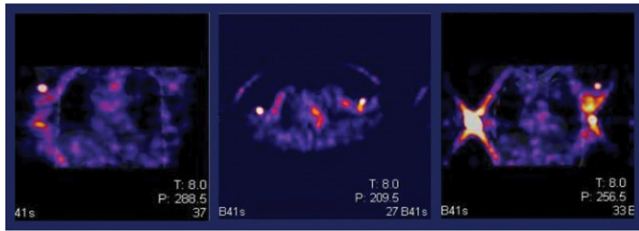


**FIGURE 1.**  $^{99m}\text{Tc}$ -tilmanocept imaging for intraoperative lymphatic mapping and sentinel lymph node biopsy. Example (left to right) coronal, transaxial, and coronal images from patients with breast cancer. This tracer looks beyond patterns of locoregional lymph node drainage to assess clearance from the injection site itself.

characteristics and PET/CT uptakes in esophageal squamous cell carcinoma patients:  $^{18}\text{F}$ -alfatide versus  $^{18}\text{F}$ -FDG” [245]. Integrins can be expressed in a range of tumor-related cells, including endothelial/stromal cells and tumor cells, and therefore may be less impacted by metabolic compensation in tumors in response to treatment or as a result of genomic variability. These researchers developed an  $\alpha_v\beta_3$  PET/CT probe to explore the relationship between clinicopathologic characteristics and SUV in primary and metastatic lymph nodes ( $\text{SUV}_{\text{LN}}$ ) in patients with esophageal squamous cell carcinoma. The integrin  $\alpha_v\beta_3$  is expressed particularly in the stroma or the vasculature of the tumor and is less likely to be phenotypically altered by changes in aggressiveness or differentiation in the tumor. The group showed excellent imaging results in comparison to  $^{18}\text{F}$ -FDG (Fig. 3). They concluded that  $\text{SUV}_{\text{LN}}$  was influenced by pathologic stage, lymph node status, and differentiation, so that  $\text{SUV}_{\text{LN}}$  may serve as a new parameter for patient stratification, with  $^{18}\text{F}$ -alfatide PET providing molecular information complementary to that of  $^{18}\text{F}$ -FDG. I look forward to seeing more data in other tumor types using this approach.

Another integrin subtype,  $\alpha_v\beta_6$ , an epithelial-specific integrin that is not expressed in normal tissue, is known to play a role in invasion and metastasis. Hausner et al. from the University of California Davis Medical Center (Sacramento, CA) reported on “First-in-human studies of [ $^{18}\text{F}$ ] $\alpha_v\beta_6$ -BP, a PET imaging probe targeting the cancer-associated integrin  $\alpha_v\beta_6$ ” [50]. In a safety, biodistribution, and dosimetry study, these researchers demonstrated  $^{18}\text{F}$ - $\alpha_v\beta_6$ -BP uptake not only in primary tumors but also in metastatic disease in patients with breast, colon, lung, or pancreatic cancer (Fig. 4). Metastatic lesions well under 1 cm were visualized. The agent was well tolerated, and the authors noted the potential clinical applications across a broad spectrum of disease types and sites.

Another interesting approach presented at this meeting was the use of a fluorinated compound for octreotide. Long et al. from Xiangya Hospital/Central South University Changsha (Hunan, China) and the University of North Carolina (Chapel Hill) reported on “A primitive study for clinical application of  $^{18}\text{F}$ -AIF-NOTA-octreotide PET/CT

in combination with  $^{18}\text{F}$ -FDG PET/CT for imaging neuroendocrine neoplasms” [48]. The feasibility study included 3 healthy volunteers and 12 patients with pathology-confirmed neuroendocrine neoplasms. The imaging differences noted between  $^{18}\text{F}$ -AIF-NOTA-octreotide and  $^{18}\text{F}$ -FDG PET/CT were, for the most part, a result of the way in which dedifferentiated disease takes up  $^{18}\text{F}$ -FDG more than octreotide. A total of 444 lesions detected were visualized by both tracers (discordance rate of 61%), and the remaining 286 lesions were detected by both tracers (concordance, 39%). Uptake of  $^{18}\text{F}$ -AIF-NOTA-octreotide was generally higher than that of  $^{18}\text{F}$ -FDG in patients with grades 1 and 2 disease, with  $^{18}\text{F}$ -FDG being somewhat higher in patients with grade 3 disease (Fig. 5). The authors concluded that a combination of  $^{18}\text{F}$ -FDG PET/CT and  $^{18}\text{F}$ -AIF-NOTA-octreotide has promising potential for staging and management of neuroendocrine neoplasms.

Receptor-based imaging has even more relevance in partnership with therapeutics. Chae et al. from the Asan Medical Center/University of Ulsan College of Medicine (Seoul, Republic of Korea) reported on “Diagnostic accuracy and safety of  $16\alpha$ -[ $^{18}\text{F}$ ]fluoro-17 $\beta$ -estradiol PET/CT for the assessment of estrogen receptor (ER) status of recurrent or metastatic lesions in patients with breast cancer: An open label, nonrandomized, phase 3 study” [487]. This study included 99 patients with ER+ metastatic breast cancer treated with first-line ER therapy. Patients were scheduled to undergo core needle biopsy or surgery of recurrent or distant metastatic breast cancer lesions within 15 days after  $^{18}\text{F}$ -FES PET/CT or had already undergone core needle biopsy of those lesions within 30 days before imaging (Fig. 6). One of the goals of the study was to determine to what extent  $^{18}\text{F}$ -FES PET/CT can predict response to ER therapy in these patients. The authors found that the high specificity of  $^{18}\text{F}$ -FES PET/CT can “reliably rule in the diagnosis of ER+ recurrent or metastatic breast cancer and thus can substitute for immunohistochemical assessment of ER status.”

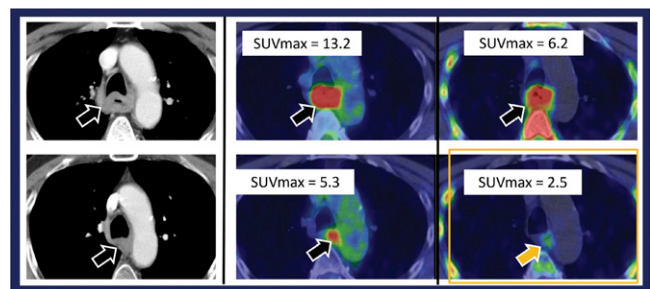


**FIGURE 2.** 4'-[methyl- $^{11}\text{C}$ ]-thiothymidine (4DST) imaging before (top row) and after (bottom row) neoadjuvant therapy for predicting therapeutic response in a patient with esophageal cancer. Left to right: CT,  $^{18}\text{F}$ -FDG PET/CT, and 4DST PET/CT. This agent can be used as a cell proliferation imaging PET tracer that incorporates directly into DNA. Post-therapeutic 4DST  $\text{SUV}_{\text{max}}$  had the most accurate diagnostic performance for predicting responses in trial participants.

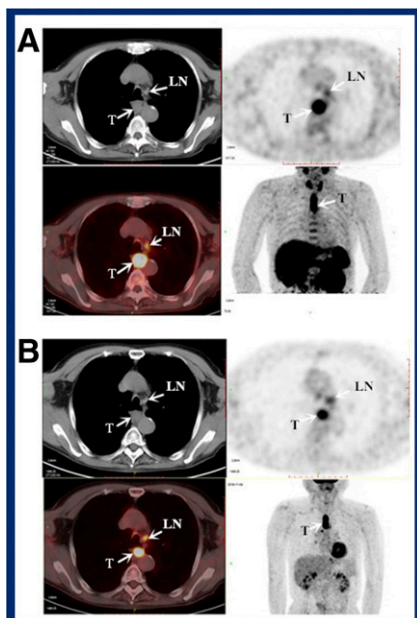


**FIGURE 3.**  $^{18}\text{F}$ -alfatide versus  $^{18}\text{F}$ -FDG uptake in patients with esophageal squamous cell carcinoma (ESCC). PET/CT images of major organs and regions of uptake at 1 h after injection of (a)  $^{18}\text{F}$ -alfatide or (b)  $^{18}\text{F}$ -FDG in a patient with upper-middle ESCC (T = primary tumor; LN = metastatic lymph node). Significant positive correlations were observed between the lymph node SUV of both tracers as well as pathologic stage, LN status, and differentiation.

The  $\alpha_v\beta_3$  PET/CT probe, which targets molecules expressed more in the stroma or the vasculature of the tumor, provided molecular information complementary to that of  $^{18}\text{F}$ -FDG.

Androgen receptor imaging has potential importance in prostate cancer, because the ability to demonstrate expression of the androgen receptor has relevance to anti-androgen therapy. This is even more relevant in the androgen splice variants that are being reported in patients with castrate-resistant disease. Vargas et al. from the Memorial Sloan Kettering Cancer Center (New York, NY), Austin Health (Melbourne, Australia), the Royal Marsden Hospital (London, UK), and the VU University Medical Center (Amsterdam, The Netherlands) reported on “Reproducibility and repeatability of quantitative  $^{18}\text{F}$ -fluorodihydrotestosterone ( $^{18}\text{F}$ -FDHT) uptake metrics in castration-resistant prostate cancer metastases: A prospective multicenter study” [86]. The study included 27 patients with 140  $^{18}\text{F}$ -FDHT-avid regions. Figure 7 shows a comparison of  $^{18}\text{F}$ -FDHT and  $^{18}\text{F}$ -FDG imaging in the same patient, with resulting imaging that is quite different for the androgen receptor tracer. The researchers found that  $^{18}\text{F}$ -FDHT imaging was highly reproducible, indicating that the tracer could be meaningfully evaluated in multiple centers with a standard protocol.

#### Molecular Imaging: Multimodality Imaging Probes

We also continue to see innovations based on the use of more than one imaging modality. Zhang et al. from the Beijing Tiantan Hospital (China), Peking Union Medical College Hospital (Beijing, China), and the National Institutes of Health (Bethesda, MD) reported on “Gastrin-releasing peptide receptor (GPPR) PET imaging with  $^{68}\text{Ga}$ -NOTA-Aca-BBN (7-14) and  $^{68}\text{Ga}$ -NOTA-IRDye800CW-BBN for evaluation of glioma patients: A prospective pilot study” [81]. This investigation included 46 patients with suspected

brain gliomas who underwent  $^{68}\text{Ga}$ -NOTA-Aca-BBN (7-14) or  $^{68}\text{Ga}$ -NOTA-IRDye800CW-BBN PET/CT or PET/MR imaging before surgery. Twenty-four of the patients also underwent infrared GPPR-targeting intraoperatively. These pilot results led the authors to conclude that “GPPR-targeting  $^{68}\text{Ga}$ -NOTA-Aca-BBN (7-14) or  $^{68}\text{Ga}$ -NOTA-IRDye800CW-BBN PET imaging provides an ideal tool for the detection of gliomas, which may also be useful for preoperative evaluation guiding surgery of glioma patients” (Fig. 8). I applaud this group for exploring this novel approach; being able to combine these 2 imaging approaches in a preoperative setting provides opportunities for improving surgical resection.

#### Molecular Imaging in Treatment Response Assessment

When exploring treatment response assessment with molecular imaging, it is crucial to be aware of the patient populations under analysis. The variables are many and complex. Tumor types have different pathologic and metabolic features that can affect treatment response, as well as impact interpretation of imaging studies. Prognostic and predictive imaging studies will have varying relevance in different patient populations. Observed metabolic changes may reflect treatment-induced changes in signaling pathways or transporter expression, and

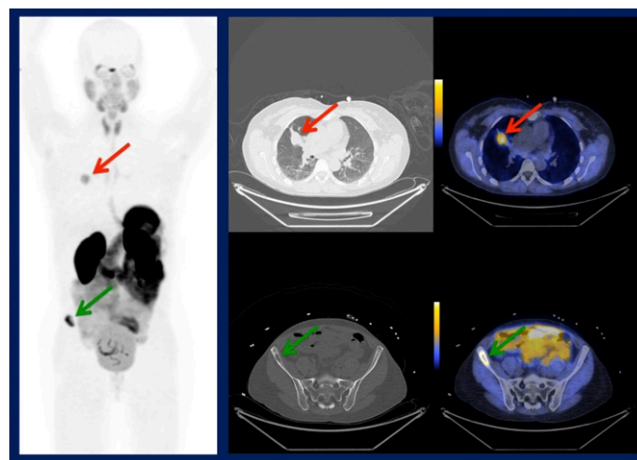


**FIGURE 4.** First-in-human study of  $^{18}\text{F}$ - $\alpha_v\beta_6$ -BP, a PET imaging probe targeting the cancer-associated integrin  $\alpha_v\beta_6$ .  $^{18}\text{F}$ - $\alpha_v\beta_6$ -BP uptake was seen not only in primary tumors but also in metastatic disease in patients with breast, colon, lung, or pancreatic cancer. Example shows a 53-year-old woman (never-smoker with no significant past medical history) who was diagnosed 20 months prior to study enrollment with stage IV adenocarcinoma of the lung. Left: Coronal maximum-intensity projection PET shows distribution of  $^{18}\text{F}$ - $\alpha_v\beta_6$ -BP 1 hour after intravenous administration. Red arrow indicates uptake in primary lung lesion; green arrow indicates metastasis in the right iliac wing. Right block: Corresponding CT (left) and PET/CT (right) images show distribution of  $^{18}\text{F}$ - $\alpha_v\beta_6$ -BP in the lung mass as well as the right iliac wing bone metastasis.

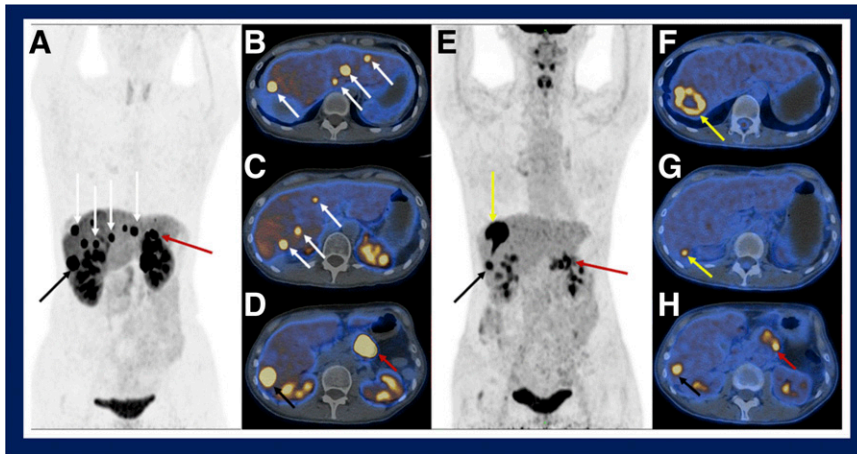


**FIGURE 5.** Clinical application of  $^{18}\text{F}$ -AIF-NOTA-octreotide PET/CT (A–D) and  $^{18}\text{F}$ -FDG PET/CT (E–H) for imaging neuroendocrine neoplasms. Imaging in a postoperative patient with pancreatic local recurrence and liver metastases shows  $^{18}\text{F}$ -AIF-NOTA-octreotide (A) and  $^{18}\text{F}$ -FDG PET (E) maximum-intensity projection images with pancreatic local recurrence (red arrows) and liver metastases (black, white, and yellow arrows). B and C:  $^{18}\text{F}$ -AIF-NOTA-octreotide PET/CT images show many intensely octreotide-avid nodules in the liver (white arrows). F and G: No corresponding  $^{18}\text{F}$ -FDG avidities were visualized, but an intensely  $^{18}\text{F}$ -FDG-avid mass was visualized in the right liver lobe (yellow arrow) and did

not demonstrate significant comparative  $^{18}\text{F}$ -AIF-NOTA-octreotide uptake, illustrating an interesting “flip-flop” phenomenon. D and H: Both tracers showed the pancreatic local recurrence (red arrows) and liver metastases (black arrows), but  $^{18}\text{F}$ -AIF-NOTA-octreotide uptake was higher than that of  $^{18}\text{F}$ -FDG. Uptake of  $^{18}\text{F}$ -AIF-NOTA-octreotide was generally higher than that of  $^{18}\text{F}$ -FDG in patients with grades 1 and 2 disease, with  $^{18}\text{F}$ -FDG being somewhat higher in patients with grade 3 disease.

different treatment approaches may have different response characteristics.

One example of the effects of this variability was presented by Lin et al. from the University of New South Wales (Sydney, Australia), the Western Sydney University School of Medicine (Australia), and Liverpool Hospital/Ingham Institute of Applied Medical Research (Liverpool), and Sunshine Coast University Hospital (all in Australia), who reported that “FDG PET/CT performed during the third week of primary radiotherapy for locally advanced human papilloma virus (HPV)–related oropharyngeal squamous cell carcinoma can predict treatment outcomes” [566]. This retrospective analysis looked at pretreatment PET and interim treatment PET (iPET) imaging results from 57 patients with newly diagnosed locally advanced disease and known HPV status (45 confirmed HPV+) treated with radical radiation therapy and concurrent systemic therapy. The authors found that the treatment response rate of nodal metastases and residual tumor metabolic burden derived from iPET in patients with HPV+ oropharyngeal squamous cell carcinoma can potentially identify those with a very low risk of treatment failure, as well as patients at intermediate-to-high risk of treatment failure, independent of HPV status. A >50% reduction in nodal metabolic tumor volume on iPET in week 3 of radiation therapy was found to provide the best predictive biomarker for treatment outcomes, particularly in the HPV+ patients.

A second example of variability in metabolic imaging in different populations came from Fuser et al. from the Mallinckrodt Institute of Radiology and Washington University in St. Louis (MO), who reported on the “Predictive value of metabolic parameters on interim  $^{18}\text{F}$ -FDG PET/CT in patients with head and neck squamous cell carcinoma (HNSCC) treated with induction chemotherapy and concurrent chemoradiation therapy” [563]. This retrospective chart study of 83 patients with inoperable stage III–IVb

HNSCC found no metabolic parameters that were predictive of overall survival. However, metabolic tumor volume and total lesion glycolysis for the primary tumor and total tumor burden were found to be predictive of progression-free survival at an  $\text{SUV}_{\text{max}}$  cutoff of 2.5 on interim PET imaging after 2 cycles of induction chemotherapy.

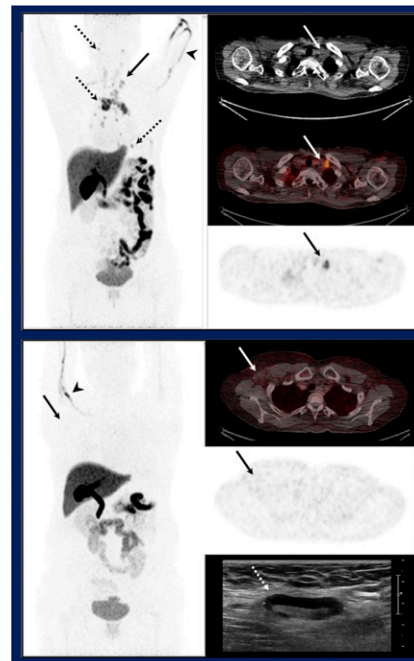


**FIGURE 6.**  $^{16}\alpha$ - $^{18}\text{F}$ -fluoro- $17\beta$ -estradiol ( $^{18}\text{F}$ -FES) PET/CT for assessment of estrogen receptor (ER) status of recurrent or metastatic lesions in patients with breast cancer. Top block:  $^{18}\text{F}$ -FES PET/CT images of a 58-y-old woman converted from ER– primary cancer to ER+ multiple metastases. Maximum-intensity projection and transaxial images show positive- $^{18}\text{F}$ -FES uptake in ER+ left supraclavicular lymph node. Positive  $^{18}\text{F}$ -FES is observed in multiple lymph nodes

in the neck, mediastinum, and pulmonary hili and pleura (dotted arrow). Bottom block:  $^{18}\text{F}$ -FES PET/CT images of a 60-year-old woman converted from ER+ primary cancer to ER– lymph node metastasis. Maximum-intensity projection and transaxial images of  $^{18}\text{F}$ -FES PET/CT show negative  $^{18}\text{F}$ -FES uptake in ER– right axillary recurrence.  $^{18}\text{F}$ -FES uptake is seen in the injected vessel of the upper extremity in both patients (arrow head).

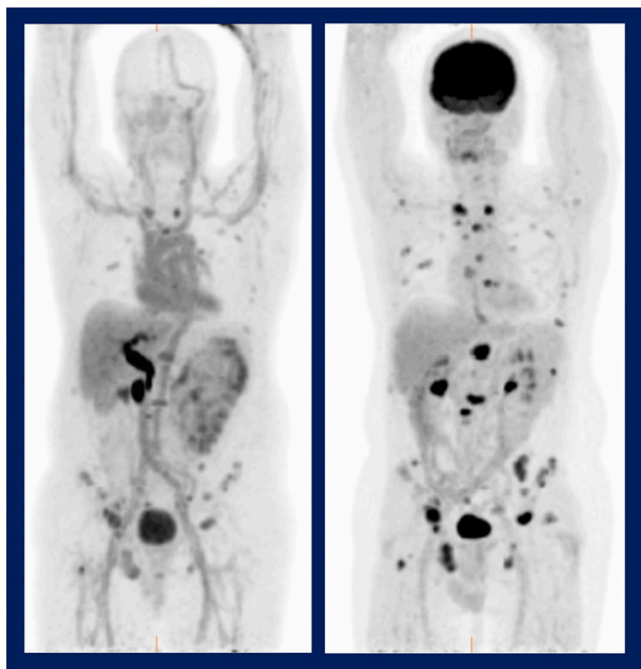


**FIGURE 7.**  $^{18}\text{F}$ -fluorodihydrotestosterone ( $^{18}\text{F}$ -FDHT) uptake (left) compared with that of  $^{18}\text{F}$ -FDG PET in a patient with castration-resistant prostate cancer. Imaging results are quite different with the 2 tracers, highlighting the heterogeneity of androgen receptor expression in metastatic disease. The researchers concluded that  $^{18}\text{F}$ -FDHT androgen receptor imaging was highly reproducible, making it suitable for multicenter trials.

Effective and informative prediction is also possible with new and more advanced therapies. Nishii et al. from the National Institute of Radiological Sciences (Chiba, Japan) reported on “Assessment of PET Response Criteria in Solid Tumors (PERCIST) of FDG PET/CT to predict progression-free survival after carbon-ion radiotherapy in patients with locally advanced pancreas cancer” [1405]. This group is among the world leaders in carbon ion therapy. The study included 19 patients who had undergone chemotherapy and who then underwent  $^{18}\text{F}$ -FDG PET/CT imaging before and 3 months after carbon ion therapy (Fig. 9). The results of Kaplan–Meier analysis of progression-free survival stratified using PERCIST showed significant differences between responders and nonresponders. These analyses indicated that a post-carbon ion therapy  $\text{SUV}_{\text{peak}}$  reduction  $>30\%$  of that before carbon ion therapy predicted early response and progression-free survival.

### Prostate Cancer Imaging and Theranostics

Prostate cancer is a very important focus of nuclear medicine research, with many presentations given at this meeting on diagnosis and therapy. Multiple PET probes (labeled with  $^{11}\text{C}$ ,  $^{68}\text{Ga}$ ,  $^{18}\text{F}$ , and others) are under investigation, as are a range of targets. Multicenter clinical trials are underway in initial staging in high-risk disease, staging following biochemical relapse, prognosis, management impact, and as part of therapeutic (theranostic) evaluation of

patients. Amid all this activity, we need to be careful to remember that competing modalities (e.g., multiparametric and whole-body MR imaging) are also being used in staging investigations. We must be cautious and careful about making confident predictions on the role that we will play in management of these patients. In addition, questions remain about applications in oligometastatic disease, appropriate management, and interpretation of equivocal results. Our armamentarium is expanding; within the last year National Comprehensive Cancer Network guidelines have added  $^{18}\text{F}$ -fluciclovine to  $^{11}\text{C}$ -choline for assessment of biochemical recurrence in prostate cancer.

I will highlight only a few of the excellent presentations on applications in prostate cancer from this meeting. Guglielmo et al. from the San Raffaele Scientific Institute (Milan, Italy), San Andrea Hospital (La Spezia, Italy), and the University of Milan Bicocca (Milan, Italy) reported on the “Effectiveness of  $^{11}\text{C}$ -choline PET/CT in predicting

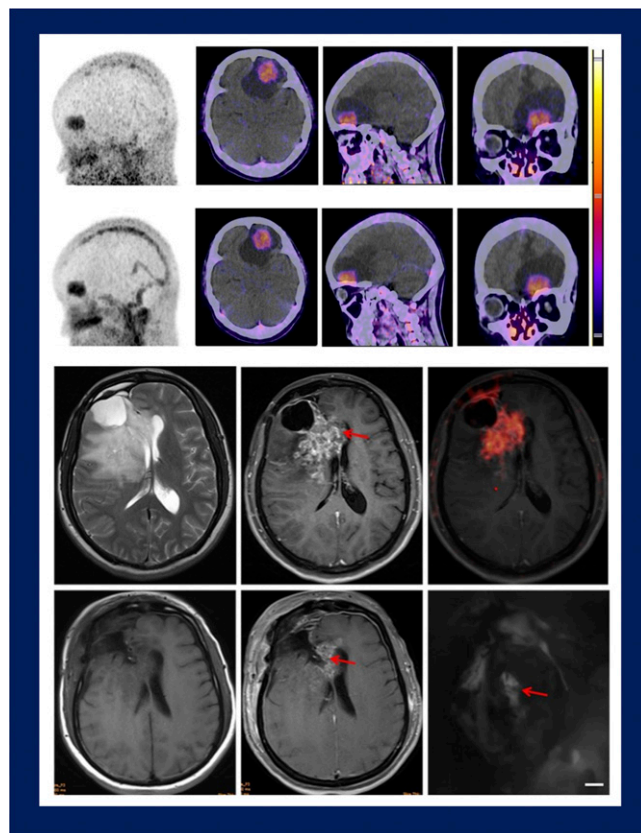


**FIGURE 8.** Gastrin-releasing peptide receptor PET imaging with both  $^{68}\text{Ga}$ -NOTA-Aca-BBN (7-14) and  $^{68}\text{Ga}$ -NOTA-IRDye800CW-BBN for evaluation of glioma patients. Top block: Similar uptakes of the  $^{68}\text{Ga}$ -NOTA-Aca-BBN (top row) and  $^{68}\text{Ga}$ -NOTA-IRDye800CW-BBN (second row) tracers on PET/CT in a newly diagnosed glioblastoma patient. Bottom block: Pre- (top row) and post- (bottom row) operative imaging in the same patient. Left to right: T1W MR imaging without contrast; T1W MR imaging with contrast; and  $^{68}\text{Ga}$ -NOTA-Aca-BBN PET imaging of residual tumor at the genu of corpus callosum with positive fluorescence.

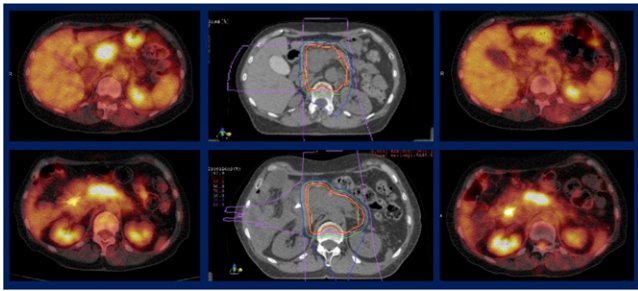


**FIGURE 9.** Assessment of  $^{18}\text{F}$ -FDG PET/CT to predict progression-free survival after carbon ion radiotherapy (CIRT) in patients with locally advanced pancreas cancer. Top row: 68-year-old man with negative disease progression at 3 months after treatment. Left to right: Before treatment, at CIRT treatment planning (55.2 Gy in 12 fractions), and at 3 months after treatment. There was no evidence of disease progression at more than 6 months after treatment. Bottom: 72-year-old woman with persistent primary site disease and peritoneal dissemination 6 months after CIRT. Left to right: Before treatment, at CIRT treatment planning (55.2 Gy in 12 fractions), and at 3 months after treatment. Study results indicated that a post-carbon ion therapy  $\text{SUV}_{\text{peak}}$  reduction  $>30\%$  of that before carbon ion therapy can predict early response and progression-free survival.

survival in prostate cancer patients with low prostate-specific antigen (PSA) biochemical relapse” [1456]. This single-site retrospective study included 210 patients with PSA serum levels  $<1$  ng/mL (mean, 0.53 ng/mL; range, 0.22–0.99 ng/mL) who underwent restaging  $^{11}\text{C}$ -choline PET/CT, with positive results in more than 20% of participants. The authors defined prostate cancer-specific survival as the period between radical prostatectomy and prostate cancer-related death. Over a mean follow-up period of 6.9 years, their results indicated that a positive  $^{11}\text{C}$ -choline PET/CT study can predict prostate cancer-specific and overall survival in patients presenting with very low PSA levels.

Numerous fluorinated compounds are under evaluation in prostate cancer. Giesel et al. from the Heidelberg University Hospital (Germany), the German Cancer Research Center (DFKZ) (Heidelberg, Germany), Memorial Sloan Kettering

Cancer Center (New York, NY), and the Technische Universität München (Germany) reported on “ $^{18}\text{F}$ -PSMA-1007 PET/CT in 166 patients with biochemical recurrence after radical prostatectomy” [459]. At presentation time, this multicenter study included 251 patients with a range of PSAs from slightly elevated to very high (0.2–228 ng/mL). The results demonstrated that the  $^{18}\text{F}$ -labeled prostate-specific membrane antigen (PSMA) agent had very good uptake and diagnostic capabilities, with a trend toward higher efficacy than  $^{68}\text{Ga}$ -PSMA ligands (as reported in published data). One of the advantages of this compound is that renal excretion is quite low, so that visualizing locoregional recurrence is much easier (Fig. 10). The authors were able to detect the presence of recurrent disease in up to 60% of patients with PSAs  $\leq 0.5$  ng/mL (higher than the detection rate with  $^{68}\text{Ga}$ -PSMA-11). In  $>70\%$  of patients with PSAs  $\leq 1$  ng/mL they were able to accurately detect the presence of recurrent disease, with an overall detection rate of 81.3%.

Dietlein et al. from the University Hospital of Cologne (Germany), the Dana-Farber Cancer Institute (Boston, MA), and the Institute of Neuroscience and Medicine Research Center Jülich (Germany) reported on “Performance of the novel  $^{18}\text{F}$ -labeled PSMA-ligand PSMA-7 for PET/CT in prostate cancer patients” [452]. The study included 124 patients assessed for biochemical recurrence, therapy monitoring of metastases, or staging of prostate cancer. Forty-nine of these patients had undergone androgen-deprivation therapy, and 51 had been scanned with other PSMA tracers. The researchers concluded that  $^{18}\text{F}$ -PSMA-7 imaging results were quite comparable to those with  $^{68}\text{Ga}$ -PSMA-11 or  $^{18}\text{F}$ -DCFPyL, as well as a number of other fluorinated compounds. In previous studies in biochemical recurrence cohorts, these authors reported a sensitivity of 74.2% for  $^{18}\text{F}$ -DCFPyL and 79.1% for  $^{68}\text{Ga}$ -PSMA-11. This study showed an 83% sensitivity for  $^{18}\text{F}$ -PSMA-7 PET/CT.  $^{18}\text{F}$ -PSMA-7 detected additional PSMA-avid lesions not visualized with other agents in patients with oligometastatic disease, with low PSA levels, and after biochemical recurrence (Fig. 11).

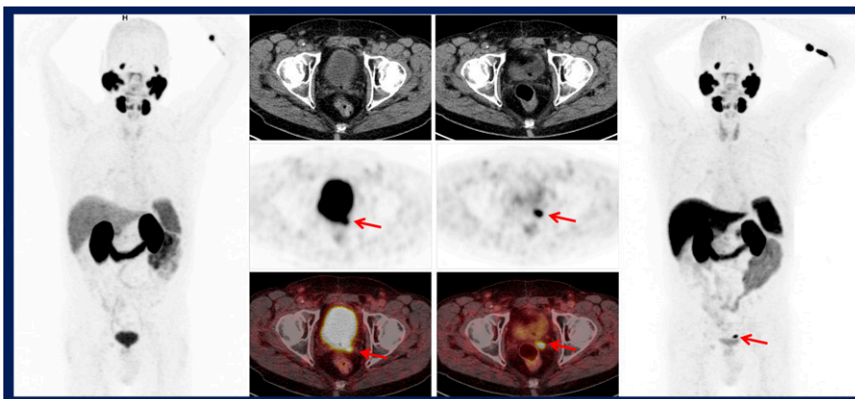


**FIGURE 10.**  $^{18}\text{F}$ -PSMA-1007 PET/CT imaging in biochemical recurrence after radical prostatectomy. Images acquired in a 76-year-old man 11 years after post-radical prostatectomy (Gleason Score 7b, pT3a, pN0), with slowly rising prostate-specific antigen value of 0.78 ng/mL. The patient underwent  $^{68}\text{Ga}$ -PSMA-11 PET/CT imaging (left block of 4 images) resulting in equivocal diagnosis of local recurrence (arrows). No definite diagnosis could be made because of adjacent high activity retention in the urinary bladder. Subsequent  $^{18}\text{F}$ -PSMA-1007 PET/CT (right block of 4 images) clearly depicted PSMA ligand uptake

in the left seminal vesicle with high contrast and very low retention in the bladder (arrows). The low renal excretion of  $^{18}\text{F}$ -PSMA-1007 was reported to facilitate easier visualization of disease.



**FIGURE 11.** Comparison of maximum-intensity projection PET/CT imaging with  $^{18}\text{F}$ -PSMA-7 and  $^{68}\text{Ga}$ -PSMA-11 in a patient with prostate cancer. Left: 60 minutes after injection of  $^{68}\text{Ga}$ -PSMA-11. Right: 150 minutes after injection of  $^{18}\text{F}$ -PSMA-7. Across this study,  $^{18}\text{F}$ -PSMA-7 detected additional PSMA-avid lesions not visualized with other agents, including in patients with oligometastatic disease, with low PSA levels, and after biochemical recurrence.

The LOCATE trial, evaluating  $^{18}\text{F}$ -fluciclovine PET/CT in patients with rising PSA levels after initial prostate cancer treatment, is an important study that was conducted at 15 sites within the United States and included a total of 213 evaluable participants. At the SNMMI Annual Meeting, Pantel et al. from the Mallinckrodt Institute of Radiology (St. Louis, MO) and the University of Pennsylvania (Philadelphia) reported on “ $^{18}\text{F}$ -fluciclovine PET/CT in patients with biochemical recurrence of prostate cancer: Impact on management and associations of clinical variables with scan findings” [457]. They demonstrated that of the 122 patients with a positive scan, management was changed for 88 (72%); of 91 patients with negative scans, management was changed for 36 (40%), for an overall management impact of 59%. This reconfirms that  $^{18}\text{F}$ -fluciclovine has a role in clinical planning in patients with biochemical relapse of prostate cancer.

### Novel Therapeutic Approaches

Remarkable progress has been made in just the last year with innovative and novel therapeutic approaches, not only with approval for  $^{177}\text{Lu}$ -DOTATATE for neuroendocrine tumors here in the United States, but also in prostate cancer. A very large number of single- and multisite trials are ongoing to assess a range of treatment regimens, different dosing regimens (e.g., constant vs de-escalating doses), scheduling changes, rechallenge treatment, and combination therapies. We also continue to watch the emergence of  $\alpha$ -particle peptide-receptor radionuclide therapy and PSMA-targeted radioligand therapy (PRLT). At the same time, these many

new approaches bring with them challenges, including the need for standardization and evidence of outcome improvements. We are also faced with accompanying economic challenges associated with many of these high-cost treatments, as well as the need for highly specialized training and general capacity building.

One group reported at this meeting on the remarkable response of patients with metastatic castrate-resistant prostate cancer to patient-specific  $^{177}\text{Lu}$ -PSMA-617 treatment. Hofman et al. from the Peter MacCallum Cancer Center (Melbourne, Australia) reported on “High activity, pain reduction, and low toxicity with  $^{177}\text{Lu}$ -PSMA-617 theranostics in metastatic castrate-resistant prostate cancer: Results of a phase II prospective trial” [531]. Thirty patients with PSMA-avid disease who had failed standard therapies received up to 4 cycles of  $^{177}\text{Lu}$ -PSMA-617 administered every 6 weeks, with a mean administered activity of 7.5 GBq per cycle. The researchers adjusted administered activities according to tumor burden, renal function, and weight in each patient. Patients were included if they had high uptake on  $^{68}\text{Ga}$ -PSMA PET/CT (defined by tumor  $\text{SUV}_{\text{max}} > 1.5$  times liver) and were excluded if  $^{18}\text{F}$ -FDG PET/CT demonstrated sites of PSMA-negative disease. Sixty-two percent of patients achieved a biochemical response of PSA reduction  $> 50\%$ . Figure 12 shows examples of the extraordinary results achieved in responders. This was named as the 2018 SNMMI Image of the Year and was recently published in *Lancet Oncology*. I look forward to seeing the results of additional multicenter studies using this exciting new therapeutic approach.

Another study looked at the influence of timing of  $^{177}\text{Lu}$ -PSMA treatment in 224 patients with metastatic prostate cancer and different previous treatment histories. Kulkarni et al. from the Zentralklinik Bad Berka (Germany) reported that “Early initiation of  $^{177}\text{Lu}$ -PSMA radioligand therapy prolongs overall survival in metastatic prostate cancer” [529]. Important observations from this study included reductions in PSA levels in 157 (70%) of patients, with a decline  $> 50\%$  in 121. The best response was complete remission with undetectable PSA. Median overall survival across the study was 27 months. It is notable that for 18 patients, the radioligand was used as first-line therapy. First-line therapy was associated with the longest overall survival (with a median not reached at 62-month follow-up). Chemotherapy-treated patients had a much shorter overall survival (median, 19 months) than chemotherapy-naïve patients (38 months), possibly reflecting comparative aggressiveness of disease. Overall survival was also shorter in patients with previous  $^{223}\text{Ra}$  treatment (17 months). The results also suggested an additive effect from combining PRLT with anti-androgen therapy. Although it is too soon to say definitively how and when this therapy can be implemented in early treatment settings, these results offer a number of intriguing potential areas for exploration.

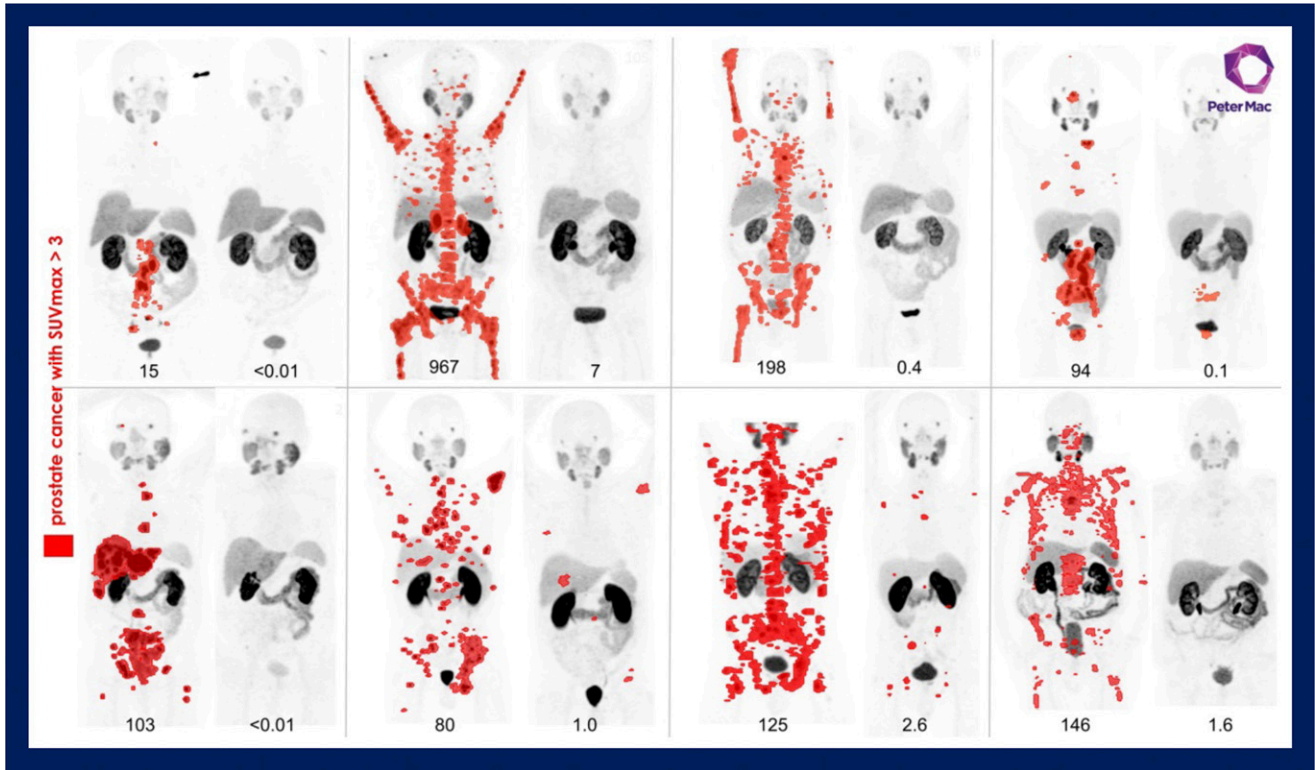


**FIGURE 12.**  $^{177}\text{Lu}$ -PSMA-617 theranostics in metastatic castrate-resistant prostate cancer. Paired  $^{68}\text{Ga}$ -PSMA-11 PET maximum-intensity projection images in 8 patients at baseline and 3 months after  $^{177}\text{Lu}$ -PSMA-617, with an overall PSA decline >98% in a prospective phase II study. Disease with SUV >3 is indicated in red. Administered activities of  $^{177}\text{Lu}$ -PSMA-617 were adjusted according to tumor burden, renal function, and weight in each patient.

Zhang et al. from Peking Union Medical College Hospital (Beijing, China), the Chinese Academy of Medical Sciences (Beijing, China) and the National Institute of Biomedical Imaging and Bioengineering (Bethesda, MD) reported on “Safety, pharmacokinetics and dosimetry of a long-lasting radiolabeled somatostatin analogue  $^{177}\text{Lu}$ -

DOTA-EB-TATE in patients with advanced metastatic neuroendocrine tumors: A phase 1 first-in-human study” [118]. This is an important study, because it shows that adapting the pharmacokinetics of DOTATATE can affect tumor concentrations of  $^{177}\text{Lu}$ -DOTA-EB-TATE, thereby improving dose to tumor. This group developed a 3-in-1

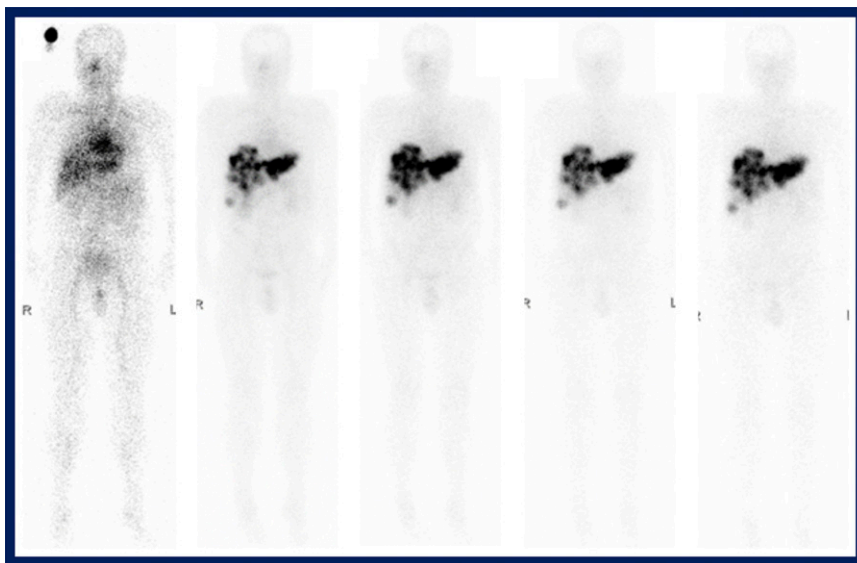


**FIGURE 13.** First-in-human  $^{177}\text{Lu}$ -DOTA-EB-TATE study in patients with advanced metastatic neuroendocrine tumors (NETs). Images acquired in a patient with advanced metastatic NET with multiple liver metastases at (left to right) 2, 24, 72, 120, and 168 hours after injection of this 3-in-1 therapeutic compound. Excellent tumor uptake in sites of metastatic NET was observed.

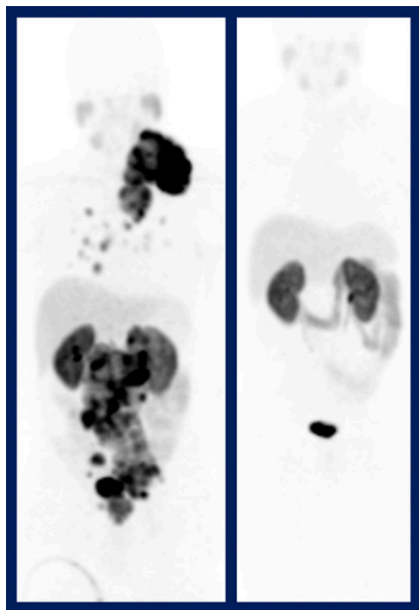


**FIGURE 14.**  $^{225}\text{Ac}$ -PSMA-617 therapy in patients with advanced-stage prostate cancer.  $^{68}\text{Ga}$ -PSMA images in a single treatment-naïve patient before (left: prostate-specific antigen = 1,301 ng/dL) and after (right: prostate-specific antigen = 0.05 ng/dL) therapy, showing remarkable response to therapy.

therapeutic compound made up of an octreotate peptide, an Evans blue motif that uses endogenous albumin as a carrier to effectively extend the half-life in the blood and increase targeted accumulation/retention within the tumor, and a therapeutic radionuclide. They reported an up to 8-fold increase in tumor dose delivery over that seen with  $^{177}\text{Lu}$ -DOTATATE (Fig. 13), although this was associated with an increase in uptake in normal organs as well, particularly in kidneys and bone marrow. I look forward to confirmation of these results from data in a larger dose-escalation study. Similar types of pharmacokinetic modifications may improve therapeutic efficacy of other agents in the future.

Pretargeting is another strategic option, with either  $\alpha$  or  $\beta$  emitters. Cheal et al. from Memorial Sloan Kettering Cancer Center (New York, NY) reported on “Pretargeted radioimmunotherapy with  $^{225}\text{Ac}$ -proteus-DOTA hapten” [123]. The researchers used a 3-step approach in which a DOTA chelator (proteus-DOTA), consisting of a free (unchelated) high-efficiency DOTA chelator for  $^{225}\text{Ac}$ , was tethered by a short polyethylene glycol linker to a  $^{175}\text{Lu}$ -complexed DOTA with picomolar affinity, thus enabling actinium delivery into tumor in a murine model. The original motivation for this research was that bone marrow toxicity is reduced with  $\alpha$  particle therapy. The “proteus” hapten is quite versatile; theoretically almost anything can be attached to the polyethylene glycol  $^{175}\text{Lu}$ -DOTA-hapten arm. This 3-arm DOTA can efficiently complex  $^{225}\text{Ac}$  and also complex  $^{111}\text{In}$  for SPECT imaging. The results showed that the  $^{225}\text{Ac}$ -proteus-hapten can be pretargeted in vivo to GPA33-expressing SW1222 human colorectal cancer xenografts with high tumor-to-blood and high tumor-to-kidney ratios. The authors concluded that “The ability to selectively deliver  $^{225}\text{Ac}$ -proteus-DOTA will greatly ex-

pand the potential of delivering precision radioimmunotherapy to human solid tumors in laboratory animals and ultimately man.” Preclinical therapy studies are currently underway.

Actinium therapy is also being explored with PSMA. Sathekge et al. from the University of Pretoria (South Africa), the University of Heidelberg (Germany), and the European Commission, Joint Research Centre (Karlsruhe Germany) reported on “Initial experience with  $^{225}\text{Ac}$ -PSMA-617 in patients with advanced-stage prostate cancer” [528]. The study included 25 patients (mean age, 66 years) with confirmed advanced-stage prostate cancer who were treated with standardized activities of 8 MBq  $^{225}\text{Ac}$ -PSMA-617 in 2-month intervals. When favorable responses were observed, activities were decreased to 6 or 4 MBq in subsequent cycles to minimize toxicity. A treatment activity of 8 MBq resulted in moderate toxicity, with grade I–II xerostomia in 28% of patients but significant antitumor response in these high-tumor-burden individuals. Remarkable antitumor activity by means of objective radiologic response or tumor marker decline was observed in 85% of evaluable patients. Figure 14 shows an example in a treatment naïve patient. Short-term results also demonstrated favorable hematologic and renal toxicity profiles and quality-of-life improvements using the decreased activities.

Langbein et al. from the Zentralklinik Bad Berka and Jena University Hospital (both in Germany) reported on “Injection of botulinum toxin for preventing salivary gland toxicity after PSMA radioligand therapy: An empiric proof

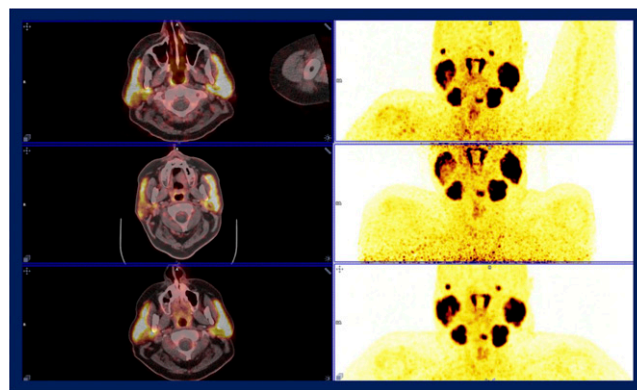


**FIGURE 15.** Botulinum toxin injection for salivary gland toxicity prevention after PSMA radioligand therapy. The first-in-human, single-patient study included a 63-year-old patient with metastatic castration-resistant prostate cancer who underwent  $^{68}\text{Ga}$ -PSMA PET/CT baseline imaging (top row), early  $^{99\text{m}}\text{Tc}$ -pertechnetate salivary gland scintigraphy after ultrasound-guided injection of 80 units of botulinum toxin into the right salivary gland (middle row), and  $^{68}\text{Ga}$ -PSMA PET/CT performed 8 months later (bottom row). PSMA imaging at 45 days (not shown) indicated a heterogeneous but highly significant reduction of radioligand uptake (up to 60% in the right compared to the left side and up to 64% compared to baseline PET/CT).

of a promising concept” [525]. In looking for a way to treat xerostomia in PSMA therapy in patients with metastatic castration-resistant prostate cancer, this group decided that instead of merely titrating the dose, they would inject botulinum toxin directly into salivary glands under ultrasound guidance. This first-in-human, single-patient study included  $^{68}\text{Ga}$ -PSMA PET/CT baseline imaging, early  $^{99\text{m}}\text{Tc}$ -pertechnetate salivary gland scintigraphy after injection of 80 units of botulinum toxin into the right salivary gland, and  $^{68}\text{Ga}$ -PSMA PET/CT performed 45 days later (Fig. 15). The 45-day PSMA imaging showed a heterogeneous but highly significant reduction of radioligand uptake (up to 60% in the right compared to the left side and up to 64% compared to baseline PET/CT). Slow recovery of uptake was noted over 8 months. The patient reported no side effects at injection or during the follow-up period. The authors concluded that “this approach could be a significant breakthrough for salivary gland protection under PSMA radioligand therapy.”

### Summary

This has been a rapid journey through some of the many outstanding presentations at this meeting. It is difficult to summarize so much original work in such a short period of

time. This is a very exciting time in which to be involved in nuclear medicine, with new discoveries and oncologic applications in molecular imaging and therapy accelerating rapidly. Some lessons are evident from these wide-ranging studies. We must be proactive in developing evidence- and outcomes-based studies for radionuclide therapies, for which we will need multicenter trials and coordinated strategies, preferably supported in some part by industry engagement. We ourselves must be thoughtful not only about how we approach patients, particularly in immunoncology, but also about our interactions with oncologists and surgeons. Strategic planning will include preparations for new programs, restructured training, reliable economic models, and pathways to implementation. New nuclear medicine researchers will be needed to continue to explore cancer biology and develop more effective therapies. Careful planning and reliable assessment are urgently needed, because as a field we are currently moving so quickly that there is a danger the train may get ahead of us. Unless we are prepared on multiple fronts, therapeutic demands in the not-too-distant future may outstrip our capacity to provide service. Nevertheless, the future is bright, and we have much to be optimistic about.

## Institute for Advanced Medical Isotopes Planned at TRIUMF, Canada’s Particle Accelerator Center

Canadian Prime Minister Justin Trudeau announced on a November 1 visit to TRIUMF (Vancouver) new funding to construct the Institute for Advanced Medical Isotopes (IAMI), a “premier centre for the life sciences that will expand Canada’s role in fast-moving advances in nuclear medicine that will improve health and save lives.” TRIUMF, which is the nation’s leading center for medical isotope research and innovation, celebrated its 50th anniversary in 2018. With support from research and clinical partners BC Cancer and the University of British Columbia, the IAMI will be a state-of-the-art facility for research into next-generation life-saving medical isotopes and radiopharmaceuticals. Located on the TRIUMF campus, it will include an integrated series of laboratories and a TR-24 medical cyclotron, one of the most technologically advanced commercial cyclotrons. In a press release, TRIUMF indicated that IAMI will offer: (1) secure isotope supplies: IAMI will secure a local supply of several important medical isotopes, including  $^{99\text{m}}\text{Tc}$ , and also enable Canadian access to the global  $^{99\text{m}}\text{Tc}$  market; (2) next-generation cancer therapies: by developing targeted radionuclide therapies for metastatic cancers, IAMI researchers will contribute to improving health outcomes and will represent Canada in this fast-growing field, as well as improve access to radionuclide therapy markets; (3) accelerated

global drug development: IAMI will provide a unique infrastructure for radiotracer production to facilitate early-stage drug development of isotope-based radiotracers; (4) improved health outcomes for Canadians: IAMI will supply additional isotopes to the TRIUMF–University of British Columbia (UBC) neuroimaging program at the Djavad Mowafaghian Centre for Brain Health (Vancouver) to bring the power of personalized medicine to more patients and boost the supply and diversity of important PET isotopes, enabling thousands of PET scans annually; and (5) industry partnerships and investment: IAMI will provide certified infrastructure for isotope production, enabling the development of new diagnostic and therapeutic substances by industry partners, and establish a powerful training platform for young researchers.

“The IAMI is a transformative project that will improve the health of Canadians. Through IAMI, TRIUMF and its partners will advance research into next-generation, life-saving medical isotopes and radiopharmaceuticals. IAMI will provide the facilities necessary to connect bench to bedside and translate scientific breakthroughs into real-world treatments for cancer and other diseases,” said Jonathan Bagger, PhD, director of TRIUMF.

TRIUMF